Recent advances in 3D printed sensors: materials, design, and manufacturing

Yijie Jiang[1]*, Md. Nurul Islam[1], Pei Dong[2], Rui He[2], Xiaozhou Huang[2], Peng-Fei Cao[3], Rigoberto C. Advincula[4,5], Narendra Dahotre[6,7], H. Felix Wu[8], Wonbong Choi[1,7]*

[1] Department of Mechanical Engineering, University of North Texas, 3940 N Elm St, Denton, TX 76207

[2] Department of Mechanical Engineering, George Mason University, 4511 Patriot Circle, Fairfax, VA 22030

[3] Chemical Sciences Division, Oak Ridge National Laboratory, Oak Ridge, TN 37831

[4] Center for Nanophase Materials and Sciences, Oak Ridge National Laboratory, Oak Ridge, TN 37830

[5] Department of Chemical and Biomolecular Engineering, University of Tennessee, Knoxville, TN 37996

[6] Center for Agile & Adaptive Additive Manufacturing

[7] Department of Materials Science and Engineering, University of North Texas, Denton, TX 76207

[8] Vehicle Technologies Office, U.S. Department of Energy, 1000 Independence Avenue Southwest, Washington, D.C. 20585

*Corresponding authors: yijie.jiang@unt.edu, wonbong.choi@unt.edu

Abstract

Sensors are of great importance in different aspects of research and industry. Future sensors will require high-efficient and low-cost manufacturing, as well as high-performance functionality in areas, such as mechanical sensing, biomedical, and optical applications. Recent advances in 3D printing open a new paradigm for sensors fabrication as a precision, customizable, and seamless process. In this article, we review the state-of-the-art 3D printing methods in sensors manufacturing and summarize the performance of the 3D printed sensing materials and devices. Special attention is paid to emerging multi-material printing and 4D printing technologies, which will benefit the fabrication of a new generation of structures with multi-functionalities. The content on 3D printed sensors covers piezoelectric sensors, medical and optical sensing devices. The performance of 3D printed sensors in comparison with the sensors made by traditional manufacturing is also covered. Finally, Conclusion and Outlook provide the viewpoints on the future development of 3D printed sensors.

Keywords: 3D printing, sensors, additive manufacturing, piezoelectric, biomedical sensors, optical sensors.

1. Introduction

3D printing, also known as additive manufacturing (AM), has gained popularity due to the great potential beyond just printing complicated prototyping structures. From being just a prototyping approach to becoming an industrial manufacturing method, these technologies have been in the market since the 1990's. Market research shows that the growth rate of 3D printing is 14.6% and the global market will reach around $35.38 billion by 2027.[1] 3D printing has been used in different environments ranging from ambient home and office use, bio-implant printing, to zero gravity space 3D printing, such as functional living organism's body parts,[2] and zero-gravity 3D printing in the international space station.[3] Apart from lab printing of delicate designs, 3D printing technology is being used for industrial[4] and construction[5] purposes. It has gained research and industrial interests in broad areas, including biomedical applications,[6,7] lightweight engineering materials,[7–10] electronics and sensors,[11] fiber composites,[8,9,12,13] and shape morphing designs.[6,14]

Among different 3D printed devices, 3D printed sensors have been attracting significant attention. In sensors manufacturing, it is important for 3D printing of complementary accessories, embedded sensing components, as well as seamless fabrication of whole sensors[15].Traditional manufacturing methods, such as coating and injection molding, are incompatible for fabricating complex structured sensors. Additive manufacturing offers unparalleled advantages in customizable and precise structural designs, as well as low waste and fast fabrication. A considerable amount of research on 3D printing of sensors, such as piezoelectric force and motion sensing, optical, and bio-medical, have been investigated in recent years[16–21]. Annual publications have increased to about 56 times for the past decade (Figure 1), according to Google Scholar search with key words "3D printing" and "sensors".

3D printed sensors are of great interest and importance in applications of manufacturing and machinery[22], automotive and aerospace[23], biomedical device[23–25], and robotics[26]. Currently, many of the reported sensors have been produced by the integration of 3D printed structures with commercial components or components made by traditional manufacturing methods[27]. Fully 3D printed and a seamless manufacturing process will be beneficial to further simplify the current multistep process, such as assembly and packaging, and therefore reduce

economic and time costs. To achieve this, main trends of developing and using multi-material 3D printing and novel 3D printable materials (e.g. responsive materials) are emerging[6,14,24,25,28–30].

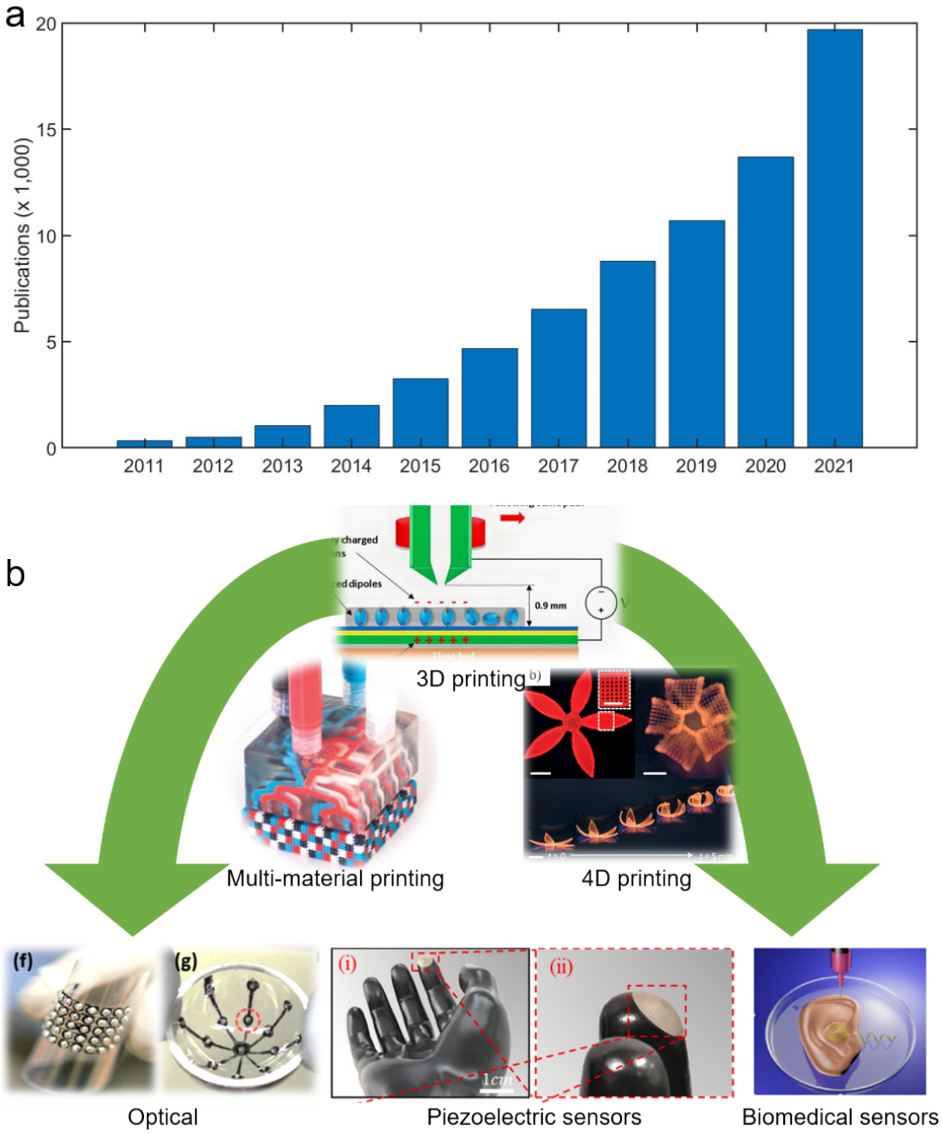

Figure 1. (a) Annual publication numbers of "3D printing" and "sensors" for the past decade. (b) Advances in 3D printing in multi-material and 4D printing, and the application in optical, piezoelectric, and biomedical sensors.[6,26,31–34]

In this article, we review the recent advances in 3D printing methods and their applications in sensors manufacturing, as well as the performance of the 3D printed materials and sensors. Although most recent reviews have extensively discussed the benefits and limitations of different manufacturing methods,[35–37] we provide a critical review emphasizing on materials, sensing

mechanism and advanced 3D printing methods followed by an outlook for the challenges and potential. This paper is structured as follows: In Section 2, individual 3D printing methods are summarized, emphasizing recent multi-material for integrated manufacturing processes (Section 2.2) and 4D printing for sensing responsive materials (Section 2.3). In Section 3, 3D printed sensor applications and their performance in mechanical, optical, and biomedical areas are reviewed. Section 4 presents the conclusion and outlook for the challenges and potential of 3D printed sensors.

2. 3D printing methods

2.1 Single 3D printing method

Major 3D printing methods can be divided into three categories, specifically extrusion-based printing, liquid resin-based printing, and powder-based printing techniques.[16,38] Table 1 lists commonly used 3D printing methods, including fused deposition modeling (FDM),[17,18] direct ink writing (DIW),[16,19] stereolithography (SLA),[39] selective laser sintering (SLS),[40] and direct energy deposition (DED),[38] grouped into the three categories.

Table 1. Summary of 3D printing methods

	3D printing methods	Printable materials
Extrusion-based	Fused deposition modeling (FDM)	Thermoplastics e.g. PLA, ABS, nylon
	3D Inkjet	Ultraviolet (UV) curable and low viscous materials
	Direct ink writing (DIW)	Elastomers, thermosets, metals and ceramics in micro/nano- particle solutions, and biomaterials
Liquid resin-based	Stereolithography (SLA)	Light (UV, LEDs, or laser) curable polymers
	Direct light processing (DLP)	
	Mask stereolithography (MSLA/LCD)	
	Two-photon lithography	

Power-based	Selective laser sintering (SLS)	Metals and alloys, polymers, and semiconductors
	Direct metal laser sintering (DMLS)	
	Direct energy deposition (DED)	
	Binder jetting	

Extrusion-based printing: FDM is the most widely used extrusion-based 3D printing method for thermoplastics,[38] such as acrylonitrile butadiene styrene (ABS) and polylactic acid (PLA). The filament is melted and extruded via a high-temperature nozzle, which has been programmed for 3D translation. The material cools down and solidifies after the extrusion and the products are manufactured in a layer-by-layer pattern. The main controlling factors[41] in FDM include the layer thickness, layer width, the printing movement, and the speed of the nozzle. Distinguished from the high-temperature melting-solidification method in FDM, DIW can print materials at room temperature and in ambient environment.[19] The printing relies on the viscoelastic non-Newtonian fluid properties in the inks. The inks are formulated to have shear thinning and yield rheological behaviors,[42] which are desired to be extruded smoothly when shear applied and maintain their shape without shear after extrusion. After DIW printing finishes, a curing procedure may be required.[16] Recently, DIW has gained huge popularity because of its capacity to room-temperature print a wide range of materials, including elastomers,[14] ceramics,[43] functional materials,[13,44] natural fiber composites,[6,13] and therefore applied in biomedical parts,[7] electronics,[45] and sensors.[11]

Liquid resin-based printing: 3D printing occurs inside a UV-sensitive liquid resin tank for a resin-based printing technique. A UV laser is shed to cure the resin locally along the printing paths or projected patterns to form a solid layer. Then the printing platform moves in the Z direction, and another resin layer is cured over the previous layer. Multiple 3D printing methods, such as stereolithography (SLA), digital light processing (DLP), and two-photon polymerization (2PP), are developed based on this mechanism[46–50]. SLA is used in the first commercially available 3D printer.[39,47]During SLA printing, a UV laser moves in the programmed path in the X-Y plane. These polymers are highly sensitive to UV irradiation and upon exposure, they quickly crosslink in this layer. Usually, the printed parts require an ultrasonic/liquid bath to remove residual resin and thermal post-curing procedures. The significant difference between the SLA and

DLP is the light source. A point-source laser light beam is used in SLA, while DLP uses the images projection in the entire platform at each layer to enhance the printing speed.

Powder-based printing: As the name suggests, powder-based 3D printing uses printing materials in powder form. A heat source, usually a high-power laser, is applied to the powders that melts and binds the powders to form solid structures. After a layer is printed, more powders are cast over the layer and the same procedure is repeated to create the next layer. The commonly used powder-based 3D printing methods include selective laser sintering (SLS), direct metal laser sintering (DMLS), and direct energy deposition (DED).[40,51] The printing technique is helpful for a wide range of materials, such as wax, polymers, metals, semiconductors. In SLS, a high-energy laser beam is used to melt and weld the powders locally to form 3D geometry in a layer-by-layer fashion. After each layer is formed, the platform is lowered, and a new layer of powders is introduced to print the next layer. The DMLS works on a similar principle to SLS with a higher energy laser beam for melting the metallic powders. Direct energy deposition (DED) is another printing method used to print high melting temperature metals and alloys. During DED, a high energy beam is used[52] for melting the wire-based or powder-based filler materials. Another advantage of DED is its capacity for repairing purposes and can be used parallel to other subtractive manufacturing methods.[52]

2.2 Multi-material 3D printing

Multi-material 3D printing (MM3DP) enables the manufacturing of multi-material, multi-part devices in a single seamless process. This fabrication technique is much simpler, faster, and cost-effective than traditional fabrication methods due to its advantages in producing minimal waste and keeping the fabrication methods into a single step. On the contrary, most electronic devices are manufactured via stacking of 2D semiconductors in conventional fabrication methods, which requires an expensive setup and leaves a considerable amount of waste. Since MM3DP allows for integrating different materials in multilayered format into a single device [6,28,30,53–55], it lifts the constraints in design, material selections, and fabrication. For example, ***Kong et al***.[54] demonstrated the potential of MM3DP by fabricating a 5-layer LED directly on the contact lens. Each layer is made from different materials and performs a distinctive function to make the LED functional. The distinct features of multi-materials AM technology to integrate other available materials to fabricate fully functional devices makes it attractive in fields like intelligent

structure[56], lightweight composites[8,13] , energy storage[53,57] and harvesting devices [29,30], flexible electronics[58,59], light emitting device[54], and sensors[14,58–60]. This section will provide critical insights into the fabrication techniques and challenges of multi-material 3D printing.

A standard method for multi-material printing is achieved via sequential switching of nozzles to deposit different materials (Figure 2a) [32,53,54,59]. Using DIW 3D printing, ***Emon et al.***[59] fabricated a 5-layer soft stretchable pressure sensor with a pressure-sensitive layer made of mild ionic liquid and polymer network film. 5 layers were printed sequentially from 3 different nozzles. Similar to pressure sensors, 3D printed batteries require multilayered structure, compromising the anode, cathode, and electrolyte to allow ions movement from anode to cathode and vice versa[53,57]. Fu et al.[53] demonstrated a fully 3D printed battery that exhibited a stable cycling performance with specific capacities of ≈160-170 mAh g^{-1}. They first printed multilayered anode with the DIW printing method, followed by electrolyte and cathode using graphene oxide-based printable inks for electrodes and solid-state electrolyte.

One major challenge of multi-material 3D printing was the slow nozzle switching rate between materials. Several nozzle designs have been investigated to address this issue, such as core-shell nozzle, actively mixing nozzle, and dual-channel nozzle (Figure 2b)[10,11,32,61,62]. Multiple materials can be printed through the same nozzle simultaneously using these structured nozzles. More recently, Skylar-Scott et al.[32] reported an extrusion-based multi-nozzle multi-material 3D printer (MM3D) that exhibits materials switching rate up to 50 Hz, which is the highest frequency reported to date (Figure 2c-d). High-frequency inks switching is achieved by applying pressure on flow channels via a high-speed pneumatic actuator. Precise tuning of ink viscosity, printing pressure, and nozzle shape are critical to avoid inks mixing and back flowing into the static channel. The reported printer ensures a distinct ink flow through the nozzle at a given time, enabling the fabrication of 3D multi-material parts in a voxelated way. The printer can accommodate maximum of 128 microfluidic nozzles, and each nozzle could be loaded with eight different inks. MM3D's unique abilities to have multiple nozzles and the high-frequency ink switching enable high-speed and high-throughput 3D printing of multi-material structures at the micrometer resolution. The author demonstrated the effectiveness of the MM3D printer by printing a soft actuating robot consisting of soft and stiff elastomers with embedded pneumatic channels. The soft actuating robot can walk and even carry weight by sequential compressing the channel.

Distinguishing from the single method of multi-material 3D printing, combining multiple printing methods into a single device has advantages in printing different materials in a seamless manufacturing process. For example, a hybrid 3D printer consisting of SLA, FDM, and DIW AM methods can use photocurable resin, PLA filament, and viscoelastic materials into one object. *Roach et al.*[63] developed a hybrid 3D printer by incorporating inkjet, FDM, DIW, and aerosol jetting. They also demonstrated the potential applications of such a system for fabricating soft actuators, stretchable light ribbons, and wiring boards. However, elucidating the curing mechanism of different materials and resolution differences between AM methods.

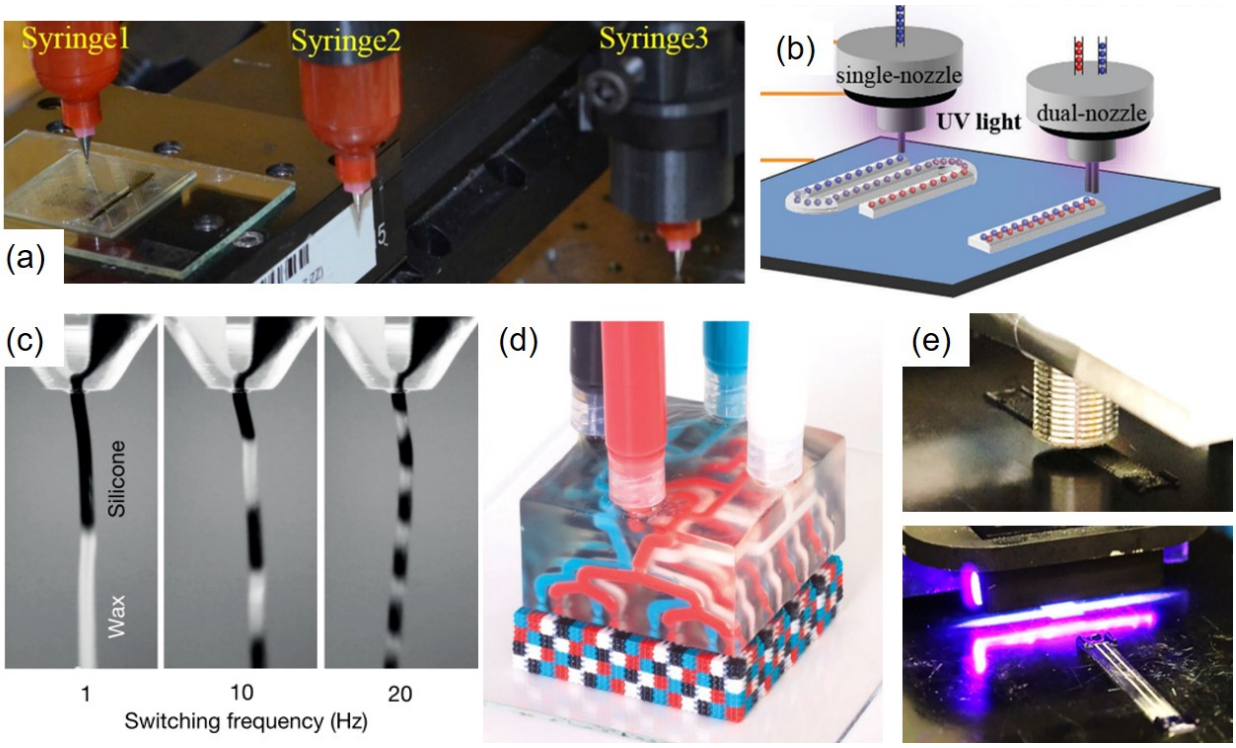

Figure 2. Multi-material 3D printing methods. (a) Switch between multiple nozzles in sequence during 3D printing;[59] (b) dual-nozzle printing for textured composites printing;[62] (c) high-frequency materials switching via single nozzle,[32] (d) high-throughput multi-material voxelated printing,[32], and (e) multi-material multi-method 3D printing of functional composites.[63]

2.3 Functional and 4D printing

4D printing introduces the concept of adding the 4th dimension on a 3D printing as defined, "the change of shape, property, and functionality from a 3D printed structure response to time or external stimulus"[64]. The responsive behavior of 4D printed structures is programed by self-

sensing and self-actuating behavior of smart materials during printing and activated via a specific or a sequence of stimuli after printing[6,14,30,55]. In recent years, this shape morphing behavior of 4D printed structure has received tremendous attention in both research and industrial communities for its numerous applications in actuator[14,55], soft robotics[65], healthcare[6,24,66] and energy[29,30]. This section summarizes the potential applications of 4D printing, emphasizing on stimuli-responsive and shape morphing mechanisms.

One major category of 4D printed structures is thermally activated self-deployable structures[28,67,68]. Impairing inkjet and projection micro-stereolithography printing method, ***Ding et al***.[67] fabricated an intelligent lattice structure from a high-stiffness shape memory polymer and a soft responsive elastomer. The soft material was programmed to contain internal stress at ambient conditions. Upon thermal activation, the stiff material became soft and allowed the soft material to release its stress. This stress relaxation triggered the shape morphing behavior. Composite stiffness increased significantly upon cooling, and deformed laminate was locked into a permanent shape (Figure 3a). ***Tian et al.***[56] printed active origami structures using inkjet AM technique to transform from one stable geometric configuration to another under a predictable load. The deployment was programed by a smart hinge embedded inside the structure while printing. In this case, the hinge is a bi-stable joint made from smart material. The smart hinge achieves local shape morphing mechanism[56] while global shape shifting behavior[67] is conserved without a hinge. ***Zarek et al.***[28] used a global shape morphing mechanism into a flexible electronics application. Using shape memory polymer, they used an SLA-based 3D printer to fabricate smart circuit boards. A printed circuit can bend its complete form upon thermal activation. To demonstrate its application in flexible electronics, LED light was inserted into SMP printed circuit, and conductive silver nanoparticle ink was used to make electrical contact between SMP and LED. The circuit remains open at atmospheric conditions. Upon heating above the glass transition temperature of the SMP, the circuit closeds and turned on the LED.

Besides thermal activation, various solvents[6,14,55,69–72] are also used as stimuli in 4D printing. In this case, the shape morphing behavior of 4D printed structures is triggered upon immersion in a solvent. ***Kokkinis et al.***[55] applied this principle to fabricated smart locker from water-swellable soft polymer ink. Its locking mechanism is programmed by the shape morphing

of cuboid, which is activated by swelling into ethyl acetate. Before swelling, cuboid walls are flat. This swelling causes convex and concave deformations by inwards and outwards bending of opposing walls of the cuboid, resulting in a reduction in the cuboid's interior size. The smart key-lock connector has potential application in soft robots and biological systems such as muscles. Anisotropic behavior (swelling and stiffness) of the cellulose fibril plays a crucial role in shape morphing in plants[73–75] which can be predicted and controlled as a function of fiber alignment[6]. The extrusion-based 3D printing technique offers excellent control over fiber orientation along the printing direction. The degree of alignment could be controlled further by tuning printing speed and nozzle diameter[13]. ***Lewis et al.***[6] made the use of extrusion-based shear-induced printing method to print viscoelastic ink, formulated from cellulose fibers and acrylamides for mimicking the dynamic morphing behavior of orchid (Figure 3b). The intelligent behavior of the composite was encoded during printing by aligning fiber along the printing direction and activated by immersing into water (Figure 3b). The hydrogel-cellulose ink was printed in a single step into orchid shaped structure with locally defined anisotropic swelling and stiffness.

Nature-inspired designs with self-sensing functionality are another potential application of 4D printing. In nature, the complex vein network of plant leaves results in dynamic morphologies via sensing their surrounding environmental conditions (e.g., humidity and temperature) to provide tree stability[76]. Numerical studies showed that plant leaf-inspired turbine blades have improved strength and stiffness, lower stress intensity, and more extended fatigue than conventional blade[77,78]. Inspired by plant leaf dynamics, ***Momeni et al.***[30] designed and fabricated a PLA-based 4D printed flexible wind turbine blade with stable reversible bend-twist coupling (BTC) by mimicking plant leaf structure. The entire blade was fabricated in one print and avoided other mechatronic systems to sense and actuate the shape morphing mechanism for blade deformation. The desired shape-shifting behavior of the blade is achieved by heating above glass transition temperature and cooling at ambient conditions. Inspired by diurnal and nocturnal flowers, ***Momeni et al.***[29] 4D printed a multi-functional smart solar collector with reversible shape-shifting capability. Most solar concentrators are designed as a fixed shape such as parabolic, hyperbolic, elliptic or V shape and require an expensive tracking device to keep sunlight perpendicular for the highest amount of energy harvesting[79,80]. The 4D printed solar collector remains in parabolic shape (Diurnal Flower) in perpendicular sunlight and changes its shape to hyperbola (Nocturnal Flower) in inclined sunlight conditions. This shape-shifting intelligence is encoded by arranging

active and passive materials via 3D printing and is responsible for a 25% optimal efficiency increase.

Furthermore, biomimetic 4D printing[6] could bring significant transformation in the medical field in applications like organ printing[66], tissue engineering[66], drug delivery vessel[24], and biomedical stent[81] fabrication. Targeted drug delivery for cancer treatment has been proven effective, but challenges remain in bioavailability, non-specific targeting, and delivery carrier for multiple drugs. Herein, 4D printing offers a promising solution to deliver drugs to a specific part of the human body. ***Malachowski et al***[24]**.** They fabricated a biphasic tissue gripper to control medicines responding to particular stimuli. The gripper is biodegradable and thermo-responsive. Drug-loaded grippers start gripping the tissue at body temperature over 32 ^{o}C and release the drug from its pores to the targeted delivery site (Figure 3c). A cardiac stent is extremely useful to supply oxygen-rich blood to heart muscle after a heart-attack[81]. But the fabrication of stent has been limited in traditional manufacturing because of its complex, patient-specific, and high-resolution design[82,83]. Here 4D printing comes in to fabricate patient-specific stent. ***Ge et al.***[81] reported a 4D printed stent with tunable diameter, height, joint numbers, ligament diameter and inter-ligament angle by using body temperature as a trigger. They programmed the stent to reduce its diameter for ease of implementation. Then the implemented stent was thermally actuated to its original shape (Figure 3d).

In summary, 3D printing has its unique advantages in manufacturing complex 3D structures, controlling internal microstructures, performing *in-situ* poling of sensor materials, embedded printing of functional units into structural materials, and achieving seamless manufacturing processes[27,55,84–86]. Compared to traditional manufacturing technology, current 3D printing technology still has technical and commercial barriers in time and economic cost and needs novel and high-performance printable materials. The developments in multi-material printing and smart materials via 4D printing are advancing to resolve these challenges.

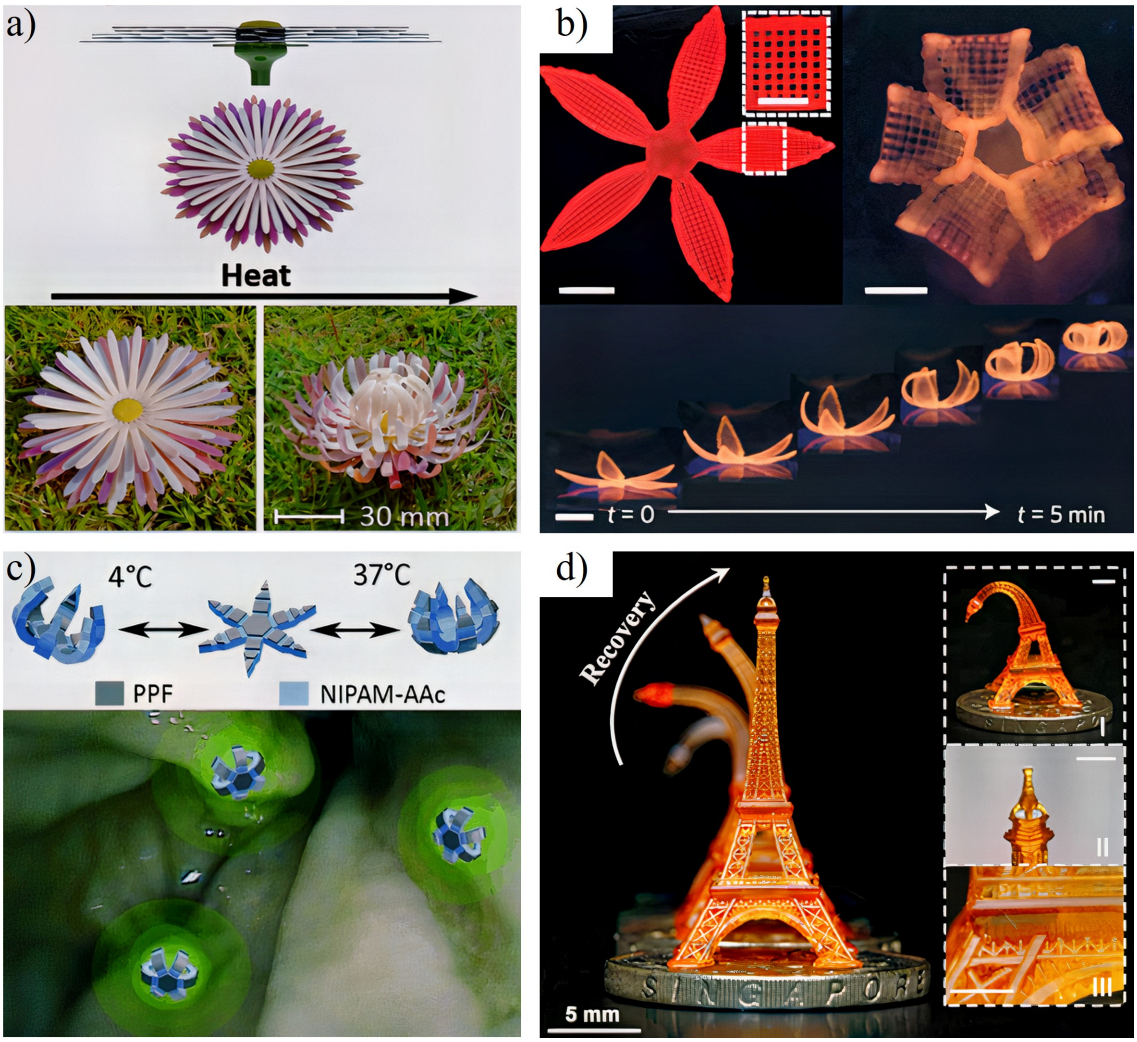

Figure 3. Sensing and responsive behaviors of 4D printed materials. a) A 4D printed multilateral flower that blooms upon heating.[67] b) Biomimetic 4D printing of a moisture responsive orchid flower and its morphing process as a function of time.[6] c) Drug delivery vessel's multi-material flower reacts opening and closing mechanism with body temperature.[24] d) Thermally activated Eiffel tower printed on a Singapore dollar.[81]

3. Applications

In this section, three categories of sensors that have been studied intensively, namely piezoelectric sensors, optical sensors, and medical sensors, are reviewed. The 3D printing methods, material properties, and performance of the 3D printed sensors are discussed.

3.1 Piezoelectric Sensors

Piezoelectric material employs the piezo effect to convert a physical quantity such as pressure, force, strain into a measurable electrical field, or vice versa.[87] Piezoelectric sensors have been extensively used in biomedical[88], biomedicine[23], wearable electronics and electronic skin[89,90], automobile[23], aerospace[23], robotics[23], ultrasonic[91], energy storage[88,92] and energy harvesting[88,93–95] based on different manufacturing processes. To date, ceramics and some polymers are widely used as piezoelectric materials. Piezoelectric ceramics such as lead zirconate titanate (PZT) and barium titanate ($BaTiO_3$) have excellent piezoelectric properties[26,85,96]. However, their poor mechanical properties, such as high brittleness and low toughness, limit their applications like flexible electronics. Although some piezoelectric polymers such as polyvinylidene fluoride (PVDF)[96,97] have limited piezoelectric properties, they offer benefits to fabricate flexible[90] and biocompatible[98] sensors. Embedding brittle but strong piezoelectric ceramics with flexible polymers is a viable approach to developing a piezoelectric sensor for flexible electronics.

Traditional piezoelectric sensor fabrication methods, including injection molding[99], melt spinning[100], spin coating[101], solution casting[102], electrospinning[103], dicing[104] and sputtering[105] are limited in fabricating piezo sensor with complex design. Three-dimensional printing has proved to be one of the most promising advanced manufacturing processes for manufacturing flexible sensors with intricate designs and tunable physical properties in multi-length scale for wearable electronics.[27,106] Currently, several 3D printing techniques such as SLA, DLP, mask-image-projection (MIP), FDM and DIW have fabricated the piezoelectric sensors. Although most recent reviews have extensively discussed the benefits and limitations of different manufacturing methods, including 3D printing in fabricating piezoelectric sensors, we provide a critical review on the performance of 3D printed piezoelectric sensors, emphasizing materials, sensing mechanism and 3D printing methods. In addition, future prospects are outlined in conclusion.

3.1.1 Photopolymerization-based 3D printing for piezoelectric sensors

For wearable electronics applications, piezoelectric sensors must be flexible, stretchable, highly sensitive, and wide operating pressure range.[87] Most solid piezoelectric materials are ceramics with brittle mechanical properties.[87] Therefore, they are not feasible to fabricate the flexible and stretchable complex 3D device.[107] To address this, polymer-based piezoelectric

materials were developed. ***Liu et al.***[26] formulated photocurable composites from highly piezoelectric boron nitride nanotube (BNNT) and polyethylene glycol diacrylate (PEGDA). They used stereolithography-based 3D printing techniques to fabricate flexible, self-powered conformal sensors. Two UV curable polymeric composites were formed from pristine BNNT and surface modified BNNT with photocurable resin. After printing, both films were poled under an electric field of 10 MV/m for 2 hours at 80°C. 3D printed sensors from modified BNNT composites showed 10 and 2 times higher relative sensitivity and piezoelectric response, respectively, than the new BNNT composite. Unlike conventional piezoelectric materials, where the piezoelectric charge constant is dictated by the intrinsic crystal structure of the constituent materials, ***Zheng et al.***[106] reported a method for tailorable piezoelectric coefficient through the spatial arrangement of a set of piezoelectric architectural units (Figure 4). Those piezoelectric ligament units are tessellated in 3D space and analyzed as a connectivity function to generate electric displacement in response to pressure. They developed highly sensitive piezoelectric inks from the surface-functionalized PZT nanoparticle and photosensitive monomer for SLA printers. After printing, printed lattices were poled under uniform electric fields. The reported material showed five times higher sensitivity oven piezoelectric polymer.

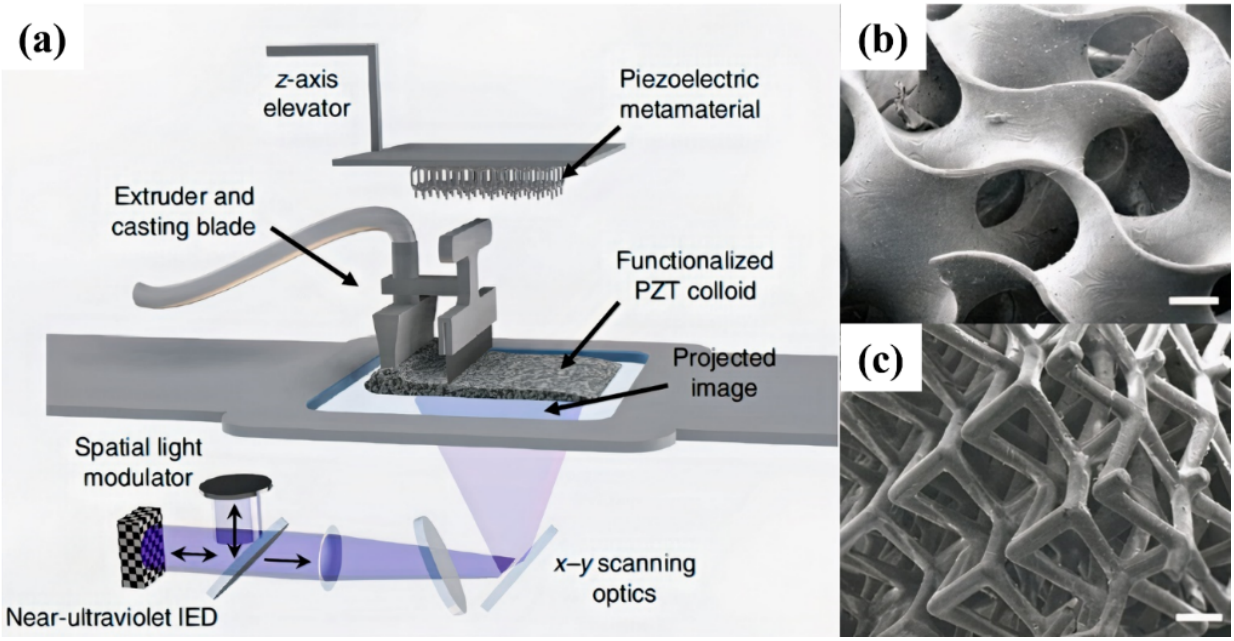

Figure 4. (a) Schematic Illustration of the High-Resolution Additive Manufacturing System. (b, c) Scanning Electron Microscope Images of 3D-Printed Piezoelectric Micro-Lattices.[106] Scale Bars, 300 μm.

Zhang et al.[108] fabricated a piezo sensor for ultrasonic sensing with the ultra-high concentration of $BaTiO_3$ (60 wt.%) using Mask-Image-Projection-based Stereolithography (MIP-SL) technology. The printable slurry consists of ceramic $BaTiO_3$ and a photocurable resin. Upon printing, printed piezoelectric elements undergo a two-step post-curing process, including organic binder removal and high-temperature sintering to achieve highly dense piezoelectric ceramics (93.7% $BaTiO_3$) with the enhanced piezoelectric response (160 pC/N). ***Zeng et al***.[91] reported a printable piezoelectric composite prepared from $BaTiO_3$ and photocurable resin (SI500). The developed UV curable composite was printed in a honeycomb structure to fabricate ultrasound sensors for biomedical application using the Mask-Image-Projection-based stereolithography (MIP-SL) process. Afterward, the photocured resin was removed, and sintering was carried out at 1350^{o}C for four hours to create dense ceramic parts. The honeycomb structured ultrasonic device showed a piezoelectric performance of 60 pC/N and an output voltage of 180 mV. ***Chen et al.***[109] fabricated annular piezoelectric arrays for ultrasonic transducer from $BaTiO_3$-SI500 photocurable composite using Mask-Image-Projection-based Stereolithography (MIP-SL). After printing, piezoelectric arrays are sintered at 1300 ^{o}C for 2 hours and poled under 30 kV/cm at 100^{o}C for 30 min. Upon postprocessing, annular arrays became mechanically robust and showed stable piezoelectric properties. Afterward, annular arrays were assembled in the ultrasonic transducer, resulting in a more extended focus zone and a smaller lateral resolution. ***Tiller et al.***[110] printed a piezoelectric microphone via digital light processing (DLP) additive manufacturing technique from photocurable piezo-composite materials. The ink consists of 33% resin, 60% $BaTiO_3$, and 1% CNT and is printed into a thin film with 27 μm resolutions using DLP. The reported 3D printed membrane was integrated into a custom-built pre-amplifier printed circuit board and resulted in a piezoelectric response of 3 pC/N.

3.1.2 Extrusion-based 3D printing for piezoelectric sensors

Extrusion-based 3D printing for piezoelectric sensors includes FDM and DIW. In FDM, the polymeric filament is melted by a heated metallic nozzle and extruded continuously. In contrast, viscoelastic ink is extruded from the nozzle due to induced shear stress in DIW 3D printing. Extruded ink is deposited layer-by-layer to form a 3D object in both cases. A piezoelectric polymeric binder is required with piezoelectric ceramics to formulate printable filament for FDM or ink for DIW. Although PVDF is inferior compared to piezoelectric ceramics in terms of piezoelectric activities, it offers intrinsic benefits of processability, flexibility, toughness,

biocompatibility, and tunable dipole moment[31,85,107]. Among four crystal orientation, i.e., α, β, γ, and δ phases, the β phase has the largest dipole moment[31,85]. In nature, it is found in non-piezoelectric α phase[31,85]. However, applying a high electric field between the nozzle and the printing bed converts PVDF from its naturally found α phase to β phase[31,85]. By applying the following technique, ***Lin et al.***[85] fabricated single-layer pressure sensors from $BaTiO_3$ composite filament using an electric poling-assisted additive manufacturing (EPAM) process. $BaTiO_3$ composite filament composed of $BaTiO_3$ and PVDF.

The effect of $BaTiO_3$ loading in the composite is investigated in terms of β phase content and piezoelectric coefficient, and the highest output current has resulted in an addition of 15% $BaTiO_3$ with PVDF, which is 1033% and 580% higher than the non-poled and poled PVDF. Both β phase content and piezoelectric coefficient increase almost linearly with $BaTiO_3$ loading. But EPAM is restricted only in fabricating single-layer piezo sensors. By addressing this limitation, ***Kim et al.***[31] proposed high electric field-based poling called corona poling process in FDM 3D printer for fabricating multi-layered pressure sensor (Figure 5a). In the reported method, a voltage of 12kV is applied between the printing bed and the nozzle tip to create a high electric field. As the electrically charged nozzle moves in preprogram printing path, this high electric field aligns the dipoles of PVDF. The β phase transformation and piezoelectric output current increase with applied voltage. The reported highest output current is 0.106 nA for applying 12kV voltage, which is 2617% higher than their previous study[85].

Fernando et al.[111] compared the piezoelectric properties of the solvent cast and 3D printed thin films, fabricated from $BaTiO_3$/PVDF nanocomposite. After fabrication, both films were subjected to a thermal poling process for 2 hours to transform the PVDF α phase to the β phase. Thermal poling enhances β phase content by 7.7% and 4.2 % for 3D printed and solvent casted thin film while 67% increase in output current for 3D printed over solvent casted thin film. ***Wilburn et al.***[96] used the FDM process to fabricate flexible capacitive sensors from PVDF, $BaTiO_3$, and CNT nanocomposite for temperature and strain sensing applications. $BaTiO_3$ enhances piezoelectricity, CNT improves di-electric and mechanical properties of PVDF. Both temperature and strain sensitivity increase with the filler content of $BaTiO_3$ and CNT until the percolation threshold. Maximal capacitance for temperature and strain sensor obtained for a comprehensive composite composition of 1.7 wt.% CNTs/60 wt.% $BaTiO_3$/PVDF and 1 wt.% CNTs/12 wt.% $BaTiO_3$/PVDF respectively.

In DIW, the ink formulation method plays a critical role in tuning the functional properties of 3D printed device[112]. ***Bodkhe et al.***[23] maximized the piezoelectric output of PVDF/$BaTiO_3$ piezo sensor by simply tuning ink formulation methods. Three different ink preparation methods, such as ball milling, screw extrusion, and sonication, were investigated, and superior piezoelectric properties were reported via ball milling. All those inks were used to fabricate cylindrical sensors using extrusion-based printing without electric poling (Figure 5b, c). The reported 3D printed non-poled sensor from ball-milled ink showed a comparable piezoelectric performance (18 pC/N) with poled PVDF sensor. Shear force induced while ink extrusion aligns the dipoles of PVDF and enhances β-phase content to 78% upon the addition of 10 wt.% $BaTiO_3$ loading. 3D printed sensor showed a 33% β-phase content increase compared to solution-film cast manufacturing technique. Using the previously reported ink formulation method of PVDF composites field[23], ***Bodkhe et al.***[86] fabricated a multilayer sensor using DIW 3D printing and *in-situ* electrical poling. The PVDF- $BaTiO_3$ (10 wt%) composites printed with *in-situ* poling led to a significant increase in specific charge (~300%) over 3D printed unpoled pure PVDF film. The printing method and ink scopes are demonstrated by printing gait-monitoring sensors on a shoe to differentiate effectively between walking and stamping.

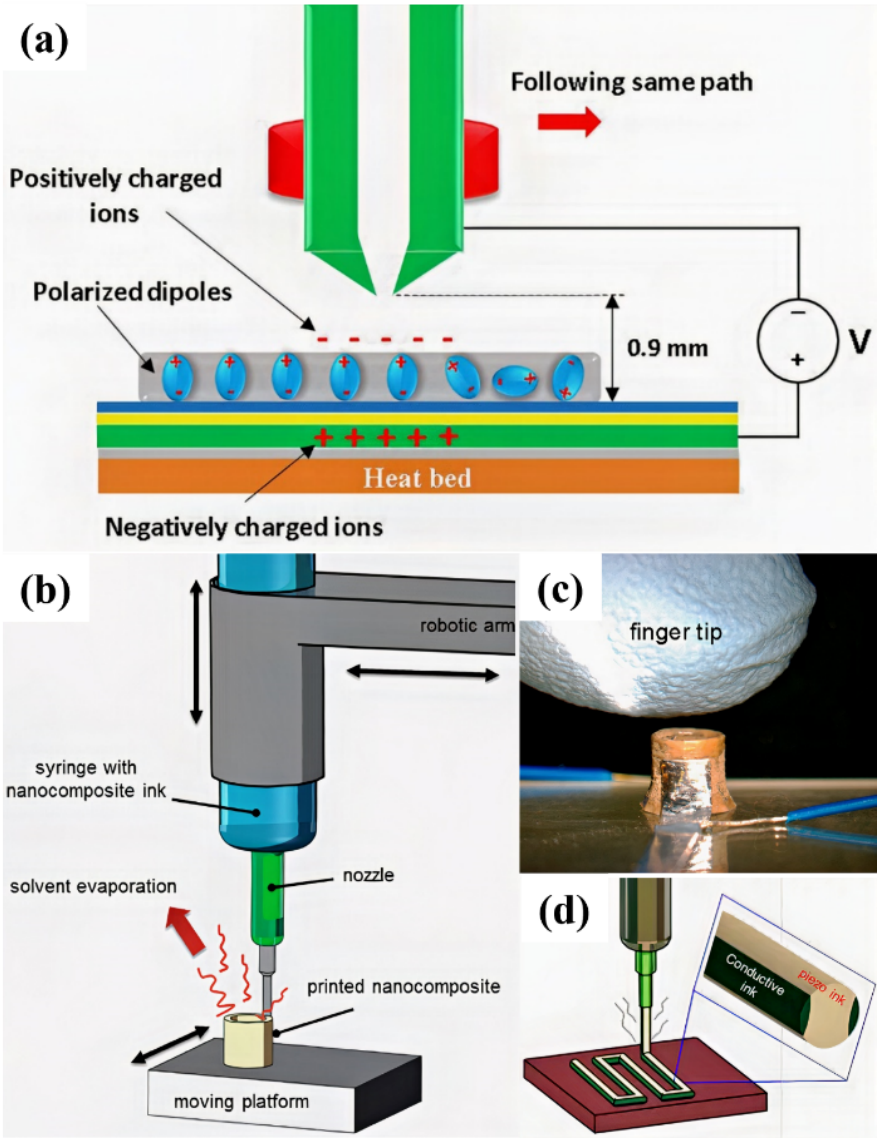

Figure 5. (a) 3D printing piezoelectric sensors with in-situ corona poling process,[31] (b) DIW printing of PVDF-$BaTiO_3$ nanocomposite.[23] (c) Finger-pap testing of PVDF-$BaTiO_3$ piezoelectric sensors.[23] (d) A schematic illustration of coextrusion embedded 3D printing.[27]

Wei et al.[88] prepared a piezo sensor from a viscoelastic paste composed of barium titanate ($BaTiO_3$), polyvinyl alcohol (PVA), and polyethylene glycol (PEG) using DIW. After printing, a two-step heat treatment process was carried out at 600 ^oC for 2 hours and 1300 ^oC for 5 hours to create a dense ceramic part, followed by a poling process under an electric field of 6 kV/cm for 4 h. The printed sensor exhibited a piezoelectric coefficient of 420 pC/N. By using bulk $BaTiO_3$, ***Marquez et al.*** [113] formulated an extrudable ink from $BaTiO_3$ and PVDF for the DIW 3D printing technique. PVDF and DMF were used as binder and plasticizer for smooth extrusion of $BaTiO_3$

while printing and removed by sintering at 1400 ^{o}C after printing. The final bulk ceramic yielded a piezoelectric coefficient of 200 pC/N. Unlike conventional 3D printing of piezoelectric sensors where a minimum of three steps are required (printing of (i) sensor element (ii) electrodes and (iii) electric poling), ***Bodkhe et al.***[27] reported a fabrication method to manufacture ready-to-use sensors in only one single manufacturing step at ambient condition (Figure 5d). They formulated printable inks from PVDF/$BaTiO_3$ for sensor elements and a conductive silver ink for electrodes. Using multi-material printing, the aero-elastic sensors were printed on miniature wings to monitor aero-elastic stability and wearable sensors for the knee joint and respiration monitoring.

Table 2. Summary of the piezo materials fabricated by additive manufacturing and traditional manufacturing

Fabrication Method	Materials	Sensing Enhancement Mechanism	Poling Condition	Piezoelectric coefficient (pC/N)	Output Voltage (V)	Output Current (nA)	Ref.
Additive Manufacturing							
SLA	0.2wt% Pristine BNNT-PEGDA	Electric Poling	10 MV/m for 2 h	d_{33}=8	0.4	NA	[26]
SLA	0.2wt% Modified BNNT-PEGDA	Electric Poling	10 MV/m for 2 h	d_{33}=14	1.1	NA	[26]
SLA	10wt% $BaTiO_3$-PEGDA	Electric Poling	10 V/μm	d_{33}=3	0.1	NA	[114]
SLA	10wt% $BaTiO_3$-PEGDA-CNT	Electric Poling	10 V/μm	d_{33}=17	0.25	NA	[114]
SLA	10wt% $BaTiO_3$-PEGDA-TMSPM	Electric Poling	10 V/μm	d_{33}=40	0.5	NA	[114]
DLP	70wt% $BaTiO_3$-Resin	Electric Poling	2 kV/cm for 30 min	d_{33}=60	0.18	NA	[91]
DLP	93.7wt%$BaTiO_3$-Resin	Electric Poling	30kV/cm for 30 min	d_{33}=160	0.3	NA	[108]
DLP	60wt% $BaTiO_3$-CNT-PEGDA	x	x	d_{33}=3	0.025	NA	[110]
FDM	PVDF	Electric Poling	13.3 Kv/mm	d_{31}=0.048	NA	0.106	[31]
FDM	PVDF	x	x	d_{33}=0.007	NA	0.0039	[85]
FDM	PVDF	Electric Poling	40 MV/m	d_{33}=0.01	NA	0.0065	[85]
FDM	15wt% $BaTiO_3$-PVDF	Electric Poling	40 MV/m	d_{33}=0.1	NA	0.0442	[85]
FDM	9wt% $BaTiO_3$-PVDF	x	x	d_{31}=0.0029	NA	0.05	[111]
FDM	9wt% $BaTiO_3$-PVDF	Electric Poling	50 MV/m for 2 hours	d_{31}=0.021	NA	0.15	[111]
FDM	PVDF	Electric Poling	3.0MV/m	x	NA	1.6	[115]
DIW	10wt% $BaTiO_3$-PVDF	x	x	d_{31}=18	2.8	NA	[23]
DIW	93wt% $BaTiO_3$-PVDF	Electric Poling	6 kV/cm for 4 h	d_{33}=420	NA	NA	[88]

DIW	71wt% $BaTiO_3$-PVDF	Sintering and electric poling	0.66 MV/m for 15 hours	d_{33}=200	NA	NA	[113]
DIW	10wt% $BaTiO_3$-PVDF	x	x	d_{31}=18	NA	NA	[27]
SLS Printing	PVDF-pBT-4Ag	Electric Poling	x	d_{33}=9	10	142	[116]
Binder Jetting	$BaTiO_3$	Electric Poling	2 kV/cm for 2 hours	d_{33}=74.1	NA	NA	[117]
Traditional Manufacturing							
Molding	94wt% BNT-BT	Sintering and electric poling	6.8 kV/mm for 30 min	d_{33}=164	8.95	NA	[118]
Molding	97wt% NKN-BNT	Sintering and electric poling	4.0 kV/mm for 30 min	d_{33}=204	10.8	NA	[119]
Casting	9wt% BaTiO3-PVDF	x	x	d_{31}=0.0074	NA	NA	[111]
Casting	9wt% $BaTiO_3$-PVDF	Sintering and electric poling	50 MV/m for 2 hours	d_{31}=0.009	NA	0.09	[111]
Casting	50vol% $BaTiO_3$-PVDF	Electric Poling	x	d_{33}=61	NA	NA	[120]
Casting	2.0Fe-RGO-PVDF	x	x	x	5.1	254	[121]
Casting	PZT-CNT-PDMS	Electric Poling	x	x	1.52	54.5	[122]
Spin Casting	12wt% $BaTiO_3$-1wt% CNT-PDMS	Electric Poling	100 kV/cm for 20 hr	x	3	300	[123]
Spin Coating	30wt% $BaTiO_3$-P(VDF-HFP)	Electric Poling	100 kV/cm for 20 h	x	5	750	[124]
Spin Coating	PVDF	Electric Poling	40 V/um for 30 min	x	2	300	[125]
Electrospinning	PVDF Fiber mat	Electric Poling	x	x	0.2	40	[126]
Electrospinning	BaTiO3-P(VDF-TrFE)	Electric Poling	x	x	6	1500	[127]
Electrospinning	P(VDF-TrFE)-10vol% NKN	Electric Poling	x	x	0.98	78	[128]
Disposition	$BaTiO_3$	Electric poling	100 kV/cm for 15 h	d_{33}=105	1	26	[129]
Spinneret Spinning	33.3wt% BaTiO3-PVC	Electric poling	3 kV/mm	d_{33}=13.7	0.9	10.5	[130]

Table 2 compares the piezoelectric properties of piezoelectric sensors produced by traditional and additive manufacturing with different compositions and sensing mechanisms. Piezoelectric properties of the piezoelectric materials largely depend on the dipole's orientation in the crystals[31,85,86]. This dipole formation process can be tuned by mechanical stretching, external electric field poling, or both. In traditional fabrication methods, the electric poling mechanism is widely used to orient dipoles after fabrication[23,85,111]. While additively manufactured, sensors can be mechanically stressed and electrically poled simultaneously, making the fabrication process simpler and more efficient. For example, non-poled PVDF-$BaTiO_3$ piezo sensors fabricated by DIW 3D printing demonstrated a piezoelectric coefficient three orders of magnitude higher than the casted materials[23,107]. Furthermore, PVDF-based poled piezo sensors, using the FDM 3D printing techniques, showed a 42.8% increase in piezoelectricity compared to non-poled sensors[85].

Among different 3D printing methods (Table 2), DIW shows its effectiveness for fabricating flexible piezoelectric sensors with tailorable piezoelectric properties and developing customizable piezoelectric materials. For the same composite composition and poling conditions, DIW printed sensors showed 6200 and 2.6 times higher piezoelectricity than those by FDM[23,107] and DLP[82,103] methods. Furthermore, each AM method has unique advantages over others. For example, photopolymerization-based 3D printing provides a high-resolution structure. In contrast, coextrusion-based DIW printing with electric *in situ* poling can fabricate ready-to-use poled sensors in a single printing process. FDM printed piezoelectric sensor is inexpensive but limited in electrical performance due to poor printing quality, print line, and resolution. To ensure a high-quality print, further optimization of melted ink's extruder geometries, heating mechanism, and flow behavior is required. Moreover, to advance the 3D printing of piezoelectric sensors, interlayer interfacial mechanisms such as material compatibility and surface roughness between layers remain explored.

3.2 Optical sensors

Optical sensors have experienced an extraordinary expansion during the last decades in both direct optical imaging and indirect optical detection areas in direct optical imaging and indirect optical detection areas in the previous decades. The core of the optical imaging system is the sensor containing a lens or camera for light transmission and image capture. The optical

imaging sensors have been widely utilized in various areas such as touch screen, mobile display[131], fire monitoring[132]. Optical detection sensors reflect the environmental transition by analyzing optical properties instead of direct optical imaging. For example, the temperature and humidity could be detected by sensing the energy loss during optical transmission[133]; the movement of visual beam position caused by refraction angle shift indicates the variation of salinity of water[134]; the sensors that could detect radiation adsorption are applied in nitrogen management for crops[135]. Being economical, highly efficient, and stable, optical sensors[136] have evolved from lab scale to massive industrial production. The sensors are pursuing a competent fabrication method. Thus, 3D printing technology has been extensively exploited in optical sensor manufacturing from a single accessory to a whole device with varieties of functions.[54,131]

3.2.1 3D printed light transmit components/accessories

As one of the most critical components inside the optical sensor, plastic optical fiber (POF) plays a role in optical transmission in optical imaging and detection sensors. Especially for optical imaging sensors, the thread usually has a complex alignment to change the direction of light. Therefore, 3D printing is an applicable technology for optical fiber design. Due to the complicated core structure owned by POF, several 3D printing technologies, including SLS, SLA, FDM, DLP, have already become a convenient and straightforward method for POF fabrication with transparent polymer filaments such as PVDF, polycarbonate (PC), and ABS.[131,137–139] ***Willis et al.***[131] explored SLA to fabricate light pipes with one transparent material (VeroClear). The benefit of the SLA technology is that the pipe's diameter could be printed as low as 0.25 mm, and the structure no longer has to be a straight line, which avoids the mechanical issue during device assembly. After installing a fiber pipe into an optical imaging sensor, the light can transform to the designed screen due to the difference of reflection index between the printed pipe and outer cladding. With 3D printed optical pipes as one part of the infrared reflecting imaging sensor, they developed chess with a display surface, which could respond to the external interaction and feedback the location on the chessboard (**figure 6a**). Additionally, 3D printed embedded components are obtained by printing the sphere and the prism structure as the front cap of the optical device. The printed part would change the direction of light transmission, and the device could be used as a lens and beam splitter (**figure 6b and c**).[131]

Most optical detection sensors request an accurate connection between the light source and POF for light signal detection, which a 3D printed accessory could easily quickly resolve. Although these 3D printed accessories don't directly participate in optical sensing, they provide extra value to the whole optical sensor due to the easy access by 3D printing to complex structures. ***Tosi et al.*** [140,141] printed the connection accessory by FDM using common polymers such as ABS and PLA. The addition can be easily mounted onto a smartphone, and POF was inserted into the acquisition through a channel. The direction of light from the smartphone to the optical sensor could be fixed. Due to the variation of light transmittance under different conditions, the device has a prior performance on hydrogen sulfide and breathing rate detection. ***Chiang et al.***[142] developed a 3D printed mold accessory for optical sensor devices in glucose concentration detection. The accessory has two parallel linear channels for a "U" shape optical probe, ensuring the easy installation and replacement for the search during the glucose concentration detection, exhibiting the advantage of 3D printing technology.

3.2.2 3D printed functional optical sensors

In addition to the light transmission component and its accessories, 3D printing technology is also applied to manufacture the main body of the sensor with various functions.

The optical path modifier is one application of a 3D printed optical device. Usually, along the optical path could enhance the sensitivity and makes the dye easier to be detected in the colorimetric analysis.[37] However, the path distance is hard to modify with the traditional sensor manufacturing method. ***Chan et al.***[143] use 3D printing to prepare a microfluidic chip containing a pump and several valves through SLA technology (figure 6d). The thickness of one layer is approximately 100μm with a 7s UV exposure period. The printed device was further immersed into ethanol and irradiated by UV light. The optical path could be easily tuned by switching the printed reaction chamber's height. The whole device could be assembled easily using a 595 nm LED light source, a smartphone camera, and a lens as an optical spectrometer. Once the specimen is pumped into the optical sensor, the image will be captured and sent to the computer for colorimetric analysis. The advantages such as low cost and easy operation ensure this optical sensor's potential to be applied in bio-detection fields.

Through multi-material printing technology, a fully 3D printed photodetector has been reported by ***Park et al.***[33]. The detector, which was manufactured through layer by layer deposition,

consists of a transparent conducting anode printed by silver nanoparticles (AgNPs) and poly(ethylene dioxythiophene): polystyrene sulfonate (PEDOT:PSS); a photoactive layer published by poly(3-hexylthiophene): 6,6-phenyl-C_{61}-butyric acid methyl ester (P3HT: PCBM); a cathode printed by liquid metal eutectic gallium indium (EGaIn) (**figure 6e**). The printed device is additionally coated with a layer of UV curing material to prevent oxidation and degradation. Due to the smooth surface ensured by layer by layer deposition, the external quantum efficiency of the printed device can be reached as high as 25.3%, which is comparable to a spin-coated device. Furthermore, due to the convenience of 3D printing technology, the limitation of substrate materials has been largely erased, indicating this photodetector could be printed on the soft or spherical substrates (**figure 6f and g**), which boost its application as an optical imaging sensor on the human body.

3D printed components are also being applied as the front cap of the optical device. ***Benjamin et al.***[20] used rubber-like materials (Tango Black+) to print the biomimetic skin as the front optical tactile sensor. The sensor also consists of a lens, LED rings, and a camera as an imaging system, ensuring comprehensive data collection. After installation onto a robot arm, the sensor exhibits excellent performance in-cylinder rolling and object moving, which can be used in car manufacturing and medical applications.

Overall, 3D printing technology has been widely utilized in optical sensor manufacturing due to its low cost, convenience, and applicability. With the development of optical sensors, increasing usage of 3D printing is expected in the future. Therefore, the category of printable materials needs to be expanded to meet the specific optical sensor requirement. For example, the printable polymer's refraction index d is considered a principal factor when 3D printing light transmission component. Thus, we expect more advanced printable material exploration for 3D-printed optical sensors.

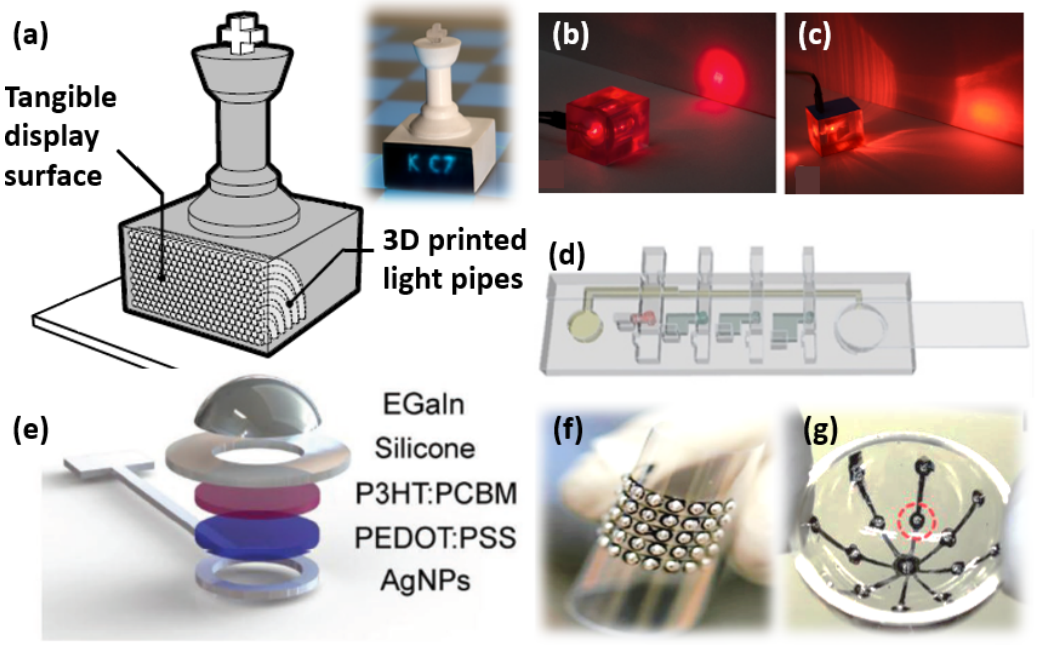

Figure 6. 3D printed optical device. (a) A schematic of 3D printed light pipes in a chess optical sensor. The insert shows the actual image of the sensor on a chessboard. (b) 3D printed lens and (c) beam splitter.[131] (d) 3D printed optical sensor for colorimetric analysis.[143] (e) A schematic of the fully 3D printed photodetector. Photodetector installation in (f) soft and (g) sphere substrates. The red circle is the actual image of the photodetector.[33]

3.3 Biomedical sensors

Several biomedical sensors have been fabricated by different 3D printing technologies as discussed above.[36,144] Compared with biomedical sensors fabricated by traditional methods, 3D printed sensors have advantages in low cost for mass production, high repeatability, and more flexibility in designing and fabrication. The materials for 3D printed sensors could be custom prepared for specific properties, such as strength and weight.[21],[145] The 3D printed sensors are also versatile in structure features, making them possess more functionalities.[146] On the other hand, some challenges still exist in 3D printed biomedical sensors, such as low biocompatibility of printing material, low reusability, and emission of the harmful nanoparticle.[36] These limitations could be mitigated by using advanced printing materials or developing new machines. In this section, some representative 3D printed biomedical sensors are introduced in three domains, including cell-based sensors, biomolecular sensors, and bionic sensors, to show how the 3D printed biomedical sensors take advantage of 3D printing technology and overcome the challenges.[147]

The first type of sensors is cell-based sensors.[21],[148],[149] A variety of information from the living cells could be detected by these sensors, such as cell imaging or toxicity detection, which is beneficial for guiding the medical diagnosis. Microscopy is a common technique to observe live cells, but it suffers from immobile, costly, and high labor requirements. To overcome the limitations, Walzik et al. developed a low-cost (less than €1250), lightweight (3.6kg), and portable time-resolved live-cell imaging sensor by desktop 3D printer (Figure 7a).[21] The device includes a digital scanning microscope, light source for imaging and corresponding sensors for temperature, gas, and humidity detection. A software interface was developed to control the entire system as well. The resolution limit of the device was up to 1.5 μm. The device could image the Haematoxylin and eosin cells at 900 overlapping locations for long-term use. It could also be adapted for some rapidly biological detections in the future.

Meanwhile, Cevenini et al. developed a smartphone-based toxicity biosensor using a desktop 3D printer.[148] As shown in Figure 7b, the adaptor was printed in a customized size to fit and be mounted on a smartphone.

The cartridge contained an array of 4-16 wells was also printed for calibration purposes. The size of all these wells was at submillimeter level. The 3D-printed cartridge was compatible with 5% DMSO model samples and actual toxicity samples. It was robust and had features ready-to-use even after being stored at 4 °C over one week. The printing process is facile and low-cost, enabling the fast production of sensor prototypes. With the help of an android App program, the sensor could examine the toxicity assay within 30 mins. Thus, desktop 3D printing is ideal for constructing the prototype and performing initial tests for the cell-based sensor.

The second type of sensor is biomolecular, such as DNA and enzyme sensors.[145,150–152] One of the main challenges for biomolecular sensors is the low biocompatibility of printing materials. To improve the performances, Tzivelekis et al. reported a 3D printed bio-device for nucleic acid amplification by using a high-resolution and low-cost DLP-SLA printing method (Figure 7c)[145]. In this work, a micro-chamber chip was printed for polymerase chain reaction (PCR), an essential process in the biology field to amplify nucleic acid sequence using a resin material. The 3D-printed microchamber PCR chip is shown in Figure 7c. To improve the biocompatibility, the chip was then treated with UV light and washed with other solvents to prevent biomolecular from adsorbing on the chip. After the posttreatment, the amplification of 75 target

sequences showed similar amplicons result as the control groups, while the un-treated fragments did not exhibit amplicon. The results indicated good functionality and PCR compatibility when using the printed components.

Meanwhile, Loo et al. reported an electrochemical DNA biosensor fabricated by the SLS method.[150] In the printing process, the stainless-steel particles were placed on the printing stage with a laser beam and fused layer-by-layer. The helical-shaped stainless-steel electrode was printed and exhibited good compatibility with DNA. Differential pulse voltammograms measured the peak current signal reduction between methylene blue and DNA to monitor the DNA hybridization. The device detected DNA with a detection range of 1-1000 nM. For enzyme-coupled sensors, Roda et al. fabricated a disposable mini-cartridge that can be used with a smartphone to detect lactate (Figure 7d)[151]. To solve a key challenge for a bio-chemiluminescence sensor that requires a highly sensitive detector, the thermoelectrically-cooled Charge-Coupled Device camera and complementary metal-oxide-semiconductor sensors were integrated into a smartphone to improve the sensitivity. Though detecting the chemiluminescence that emitted from the reaction between lactate oxidase and horseradish peroxidase, the sensor was able to see the lactate in oral fluid and sweat with the detection limits of 0.5 mmol/L and 0.1 mmol/L, respectively. This biosensor could also potentially detect other clinical analytes in oral fluid and labor.

The third type of sensor is a bionic sensor, a sensing platform for detecting external stimuli[34,153,154] that can be used in soft robotics and improve human capabilities in different situations. One of the typical mechanical sensors is the strain sensor, which can monitor external deformations, detect human motions, and provide more options in biomedical diagnosis. Xiao et al. developed a flexible strain sensor made of multi-walled carbon nanotubes (MWCNT) and elastomer composite materials (Figure 7e).[153] The elastomer was stretchable and made of epoxy aliphatic acrylate and aliphatic urethane diacrylate. The composite material was UV-curable to be printed by the DLP technique. The sensor delivered the best performance when it contained 2 wt% MWCNT, and its detectable strain ranged from 0.01% to 60% with high mechanical durability (10 000 cycles). It also had a linear correlation to humidity and temperature, which made the sensor could be used in more practical situations.

Suppose the sensor was connected to a flexible near-field communication circuit. In that case, it could be used to detect human motion, such as detecting finger bending by adhering the

sensor to the finger joint. It is expected that the motion sensor would be a crucial part of some larger bionic devices. Besides, 3D printing could also enhance the performance of electronic bionic ears. Compared with traditional electronic devices that were two-dimensional interconnected with biological tissue, 3D printed bionic ears could three-dimensional connect biological tissue to electronics devices as it could rapidly create computer-aided design 3D modeling structure. For instance, Mannoor et al. generated a 3D-printed bionic ear using a cell-seeded hydrogel matrix.[34] As shown in Figure 7f, the bionic ear combined with a conducting polymer containing silver nanoparticles to transmit the signal. The printed ear could sense the wave in the frequencies range from 1 MHz to 5 GHz and could listen to some stereo audio music if using another complimentary ear. It is expected that this work would provide more options for humans in the bionic field.

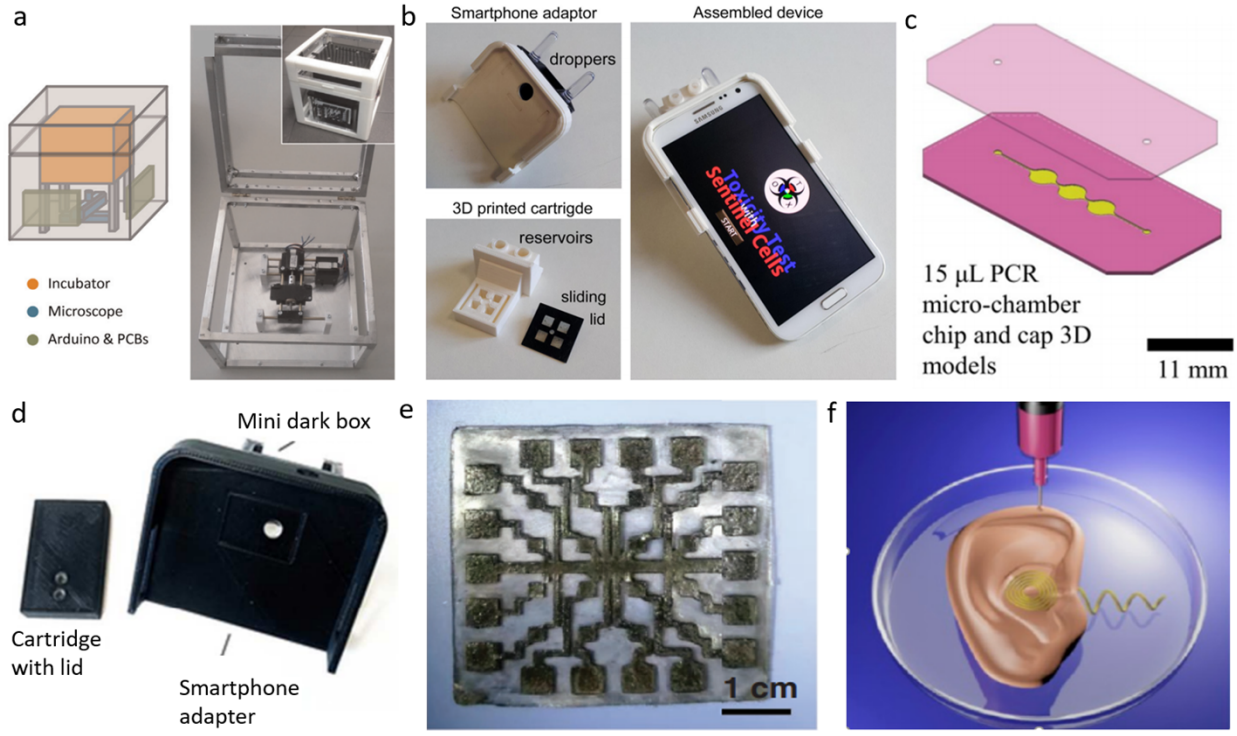

Figure 7. 3D-printed biomedical sensors. (a) A portable live-cell imaging sensor.[21] (b) 3D printed cartridge for toxicity sensors.[148] (c) A bio-device for nucleic acid amplification.[145] (d) A 3D-printed cartridge-lid adapter of smartphone for lactate sensing.[151] (e) A strain sensor 3D printed by MWCNT and elastomer composites.[153] (f) A 3D-printed bionic ear.[34]

Conclusions and outlook

With the rapid development of 3D printing technology for decades, numerous sensing materials and sensor devices manufactured by 3D printing have been demonstrated. The significant advantages, including the flexibility to print complex structures and embedded printing, make 3D printing a promising technology for manufacturing advanced sensors. The recent advances of multi-material printing in a seamless process and 4D functional printing also show great potential to overcome existing challenges. Although 3D printed sensors achieved many advantages, some challenges to be focused on are:

1. Manufacturing time and economic cost: Unlike mass production by traditional manufacturing (e.g., roll to roll process), 3D printing is in its infancy to become a batch production technology. The endeavor to research high-speed 3D printing and multi-nozzle 3D printing systems is reported, potentially improving productivity and reducing time and cost significantly.

2. Printing quality and scaling: As 3D printing is a layer-by-layer process, weak interfaces may exist between layers and residual stresses caused by the temperature profile in each layer. Control of uniformity of both macro surface topology and microstructures (such as nanoparticles dispersion) remains challenging.

3. Printable high-performance and functional materials: It is crucial to have 3D printable materials with high functionality and interfacial compatibility with other structural materials to manufacture the sensors. Advanced materials, such as micro-architected materials and nanoparticle composites, have been reported for enhanced sensing functionality under different responsive sources. By harnessing the multi-material printing or 4D printing, it is promising to address the challenges further and fabricate complete sensor devices seamlessly.

4. Utilization of high-performance computing (HPC): The online layer time control for large-scale additive manufacturing could be implemented to reduce the thermal residual stress effect. One could use an optimization framework by combining simulation and real-time feedback using thermal images. Utilization of HPC to couple the data-driven model with thermal simulation can better predict layer temperature profiles, improve the throughput of large-scale additive manufacturing and material utilization, and reduce its energy input.

References

[1] "https://www.grandviewresearch.com/press-release/global-3d-printing-market," **n.d.**

[2] M. A. Skylar-Scott, S. G. M. Uzel, L. L. Nam, J. H. Ahrens, R. L. Truby, S. Damaraju, J. A. Lewis, *Sci. Adv.* **2019**, *5*, eaaw2459.

[3] J. Ellis, N. E. Mavromatos, D. V. Nanopoulos, A. S. Sakharov, *Nature* **2004**, *428*, 6981.

[4] H. Al Jassmi, F. Al Najjar, A. H. I. Mourad, *IOP Conf. Ser. Mater. Sci. Eng.* **2018**, *324*, DOI 10.1088/1757-899X/324/1/012088.

[5] A. Paolini, S. Kollmannsberger, E. Rank, *Addit. Manuf.* **2019**, *30*, 100894.

[6] A. S. Gladman, E. A. Matsumoto, R. G. Nuzzo, L. Mahadevan, J. A. Lewis, *Nat. Mater.* **2016**, *15*, 413.

[7] K. Lin, R. Sheikh, S. Romanazzo, I. Roohani, *Materials (Basel).* **2019**, *12*, 2660.

[8] B. G. Compton, J. A. Lewis, *Adv. Mater.* **2014**, *26*, 5930.

[9] J. T. Muth, P. G. Dixon, L. Woish, L. J. Gibson, J. A. Lewis, *Proc. Natl. Acad. Sci.* **2017**, *114*, 1832.

[10] J. Mueller, J. R. Raney, K. Shea, J. A. Lewis, *Adv. Mater.* **2018**, *30*, 1705001.

[11] A. Frutiger, J. T. Muth, D. M. Vogt, Y. Mengüç, A. Campo, A. D. Valentine, C. J. Walsh, J. A. Lewis, *Adv. Mater.* **2015**, *27*, 2440.

[12] J. R. Raney, B. G. Compton, J. Mueller, T. J. Ober, K. Shea, J. A. Lewis, *Proc. Natl. Acad. Sci.* **2018**, *115*, 1198.

[13] Y. Jiang, J. R. Raney, *Adv. Mater. Technol.* **2019**, 1900521.

[14] Y. Jiang, L. M. Korpas, J. R. Raney, *Nat. Commun.* **2019**, *10*, 128.

[15] E. MacDonald, R. Wicker, *Science* **2016**, *353*, aaf2093.

[16] R. L. Truby, J. A. Lewis, *Nature* **2016**, *540*, 371.

[17] Z. Liu, Y. Wang, B. Wu, C. Cui, Y. Guo, C. Yan, *Int. J. Adv. Manuf. Technol.* **2019**, *102*, 2877.

[18] Y. Song, Y. Li, W. Song, K. Yee, K. Y. Lee, V. L. Tagarielli, *Mater. Des.* **2017**, *123*, 154.

[19] J. Cesarano, *Mater. Res. Soc. Symp. - Proc.* **1999**, *542*, 133.

[20] B. Ward-Cherrier, N. Pestell, L. Cramphorn, B. Winstone, M. E. Giannaccini, J. Rossiter,

N. F. Lepora, *Soft Robot.* **2018**, *5*, 216.

[21] M. P. Walzik, V. Vollmar, T. Lachnit, H. Dietz, S. Haug, H. Bachmann, M. Fath, D. Aschenbrenner, S. Abolpour Mofrad, O. Friedrich, D. F. Gilbert, *Biosens. Bioelectron.* **2015**, *64*, 639.

[22] Y. Zeng, L. Jiang, Y. Sun, Y. Yang, Y. Quan, S. Wei, G. Lu, R. Li, J. Rong, Y. Chen, Q. Zhou, *Micromachines* **2020**, *11*, 713.

[23] S. Bodkhe, G. Turcot, F. P. Gosselin, D. Therriault, *ACS Appl. Mater. Interfaces* **2017**, *9*, 20833.

[24] K. Malachowski, J. Breger, H. R. Kwag, M. O. Wang, J. P. Fisher, F. M. Selaru, D. H. Gracias, **2014**, 8183.

[25] H. Y. Jeong, B. H. Woo, N. Kim, Y. C. Jun, *Sci. Rep.* **2020**, *10*, 6258.

[26] J. Zhang, S. Ye, H. Liu, X. Chen, X. Chen, B. Li, W. Tang, Q. Meng, P. Ding, H. Tian, X. Li, Y. Zhang, P. Xu, J. Shao, *Nano Energy* **2020**, *77*, 105300.

[27] S. Bodkhe, C. Noonan, F. P. Gosselin, D. Therriault, *Adv. Eng. Mater.* **2018**, *20*, 1800206.

[28] M. Zarek, M. Layani, I. Cooperstein, E. Sachyani, D. Cohn, S. Magdassi, *Adv. Mater.* **2016**, *28*, 4449.

[29] F. Momeni, J. Ni, *Renew. Energy* **2018**, *122*, 35.

[30] F. Momeni, S. Sabzpoushan, R. Valizadeh, M. R. Morad, X. Liu, J. Ni, *Renew. Energy* **2019**, *130*, 329.

[31] H. Kim, F. Torres, Y. Wu, D. Villagran, Y. Lin, T.-L. Tseng, *Smart Mater. Struct.* **2017**, *26*, 085027.

[32] M. A. Skylar-Scott, J. Mueller, C. W. Visser, J. A. Lewis, *Nature* **2019**, *575*, 330.

[33] S. H. Park, R. Su, J. Jeong, S. Z. Guo, K. Qiu, D. Joung, F. Meng, M. C. McAlpine, *Adv. Mater.* **2018**, *30*, 1.

[34] M. S. Mannoor, Z. Jiang, T. James, Y. L. Kong, K. A. Malatesta, W. O. Soboyejo, N. Verma, D. H. Gracias, M. C. McAlpine, *Nano Lett.* **2013**, *13*, 2634.

[35] Y. Xu, X. Wu, X. Guo, B. Kong, M. Zhang, X. Qian, S. Mi, W. Sun, *The Boom in 3D-*

Printed Sensor Technology, **2017**.

[36] T. Han, S. Kundu, A. Nag, Y. Xu, *Sensors (Switzerland)* **2019**, *19*, DOI 10.3390/s19071706.

[37] A. Lambert, S. Valiulis, Q. Cheng, *ACS Sensors* **2018**, *3*, 2475.

[38] T. D. Ngo, A. Kashani, G. Imbalzano, K. T. Q. Nguyen, D. Hui, *Compos. Part B Eng.* **2018**, *143*, 172.

[39] D. W. Rosen, *BioNanoFluidic MEMS* **2007**, 175.

[40] S. Kumar, *Jom* **2003**, *55*, 43.

[41] O. A. Mohamed, S. H. Masood, J. L. Bhowmik, *Adv. Manuf.* **2015**, *3*, 42.

[42] A. M'Barki, L. Bocquet, A. Stevenson, *Sci. Rep.* **2017**, *7*, 1.

[43] J. Maurath, N. Willenbacher, *J. Eur. Ceram. Soc.* **2017**, *37*, 4833.

[44] J. A. Lewis, J. E. Smay, J. Stuecker, J. Cesarano, *J. Am. Ceram. Soc.* **2006**, *89*, 3599.

[45] S. L. Morissette, J. A. Lewis, P. G. Clem, J. Cesarano, D. B. Dimos, *J. Am. Ceram. Soc.* **2001**, *84*, 2462.

[46] H. Kodama, *Rev. Sci. Instrum.* **1981**, *52*, 1770.

[47] C. W. Hull, *Apparatus for Production of Three-Dmensonal Objects By Stereo Thography*, **1986**.

[48] Brian H. Cumpston, Sundaravel P. Ananthavel, Stephen Barlow, Daniel L. Dyer, Jeffrey E. Ehrlich, Lael L. Erskine, Ahmed A. Heikal, I.-Y. Sandy Lee, Stephen M. Kuebler, Dianne McCord-Maughon, Jinqui Qin, PErry, *Nature* **1999**, *398*, 51.

[49] C. Sun, N. Fang, D. M. Wu, X. Zhang, *Sensors Actuators, A Phys.* **2005**, *121*, 113.

[50] J. R. Tumbleston, D. Shirvanyants, N. Ermoshkin, A. R. Johnson, D. Kelly, K. Chen, R. Pinschmidt, P. Jason, A. Ermoshkin, E. T. Samulski, J. M. Desimone, A. R. Johnson, D. Kelly, K. Chen, R. Pinschmidt, A. Ermoshkin, T. Edward, *Science* **2015**, *347*, 1349.

[51] T. Duda, L. V. Raghavan, *IFAC-PapersOnLine* **2016**, *49*, 103.

[52] A. Dass, A. Moridi, *Coatings* **2019**, *9*, 418.

[53] K. Fu, Y. Wang, C. Yan, Y. Yao, Y. Chen, J. Dai, S. Lacey, Y. Wang, J. Wan, T. Li, Z. Wang, Y. Xu, L. Hu, *Adv. Mater.* **2016**, *28*, 2587.

[54] Y. L. Kong, I. A. Tamargo, H. Kim, B. N. Johnson, M. K. Gupta, T. W. Koh, H. A. Chin, D. A. Steingart, B. P. Rand, M. C. McAlpine, *Nano Lett.* **2014**, *14*, 7017.

[55] D. Kokkinis, M. Schaffner, A. R. Studart, *Nat. Commun.* **2015**, *6*, 8643.

[56] T. Chen, J. Mueller, K. Shea, *Sci. Rep.* **2017**, *7*, 45671.

[57] K. Sun, T. S. Wei, B. Y. Ahn, J. Y. Seo, S. J. Dillon, J. A. Lewis, *Adv. Mater.* **2013**, *25*, 4539.

[58] S. Z. Guo, K. Qiu, F. Meng, S. H. Park, M. C. McAlpine, *Adv. Mater.* **2017**, *29*, 1701218.

[59] M. O. F. Emon, F. Alkadi, D. G. Philip, D.-H. H. Kim, K.-C. C. Lee, J.-W. W. Choi, *Addit. Manuf.* **2019**, *28*, 629.

[60] M. Zhu, M. Xie, X. Lu, S. Okada, S. Kawamura, *Nano Energy* **2020**, *73*, 104772.

[61] T. J. Ober, D. Foresti, J. A. Lewis, *Proc. Natl. Acad. Sci. U. S. A.* **2015**, *112*, 12293.

[62] X. Li, J. M. Zhang, X. Yi, Z. Huang, P. Lv, H. Duan, *Adv. Sci.* **2019**, *6*, 1800730.

[63] D. J. Roach, C. M. Hamel, C. K. Dunn, M. V. Johnson, X. Kuang, H. J. Qi, *Addit. Manuf.* **2019**, *29*, 100819.

[64] Y. Tang, B. Dai, B. Su, Y. Shi, *Front. Mater.* **2021**, *8*, 658046.

[65] D. Rus, M. T. Tolley, *Nature* **2015**, *521*, 467.

[66] A. Isaacson, S. Swioklo, C. J. Connon, *Exp. Eye Res.* **2018**, *173*, 188.

[67] Z. Ding, C. Yuan, X. Peng, T. Wang, H. J. Qi, M. L. Dunn, *Sci. Adv.* **2017**, *3*, e1602890.

[68] Q. Ge, H. J. Qi, M. L. Dunn, *Appl. Phys. Lett.* **2013**, *103*, 131901.

[69] S. Tibbits, *Archit. Des.* **2014**, *84*, 116.

[70] A. Le Duigou, M. Castro, R. Bevan, N. Martin, *Mater. Des.* **2016**, *96*, 106.

[71] S. Naficy, R. Gately, R. Gorkin, H. Xin, G. M. Spinks, *Macromol. Mater. Eng.* **2017**, *302*, 1600212.

[72] D. G. Shin, T. H. Kim, D. E. Kim, *Int. J. Precis. Eng. Manuf. - Green Technol.* **2017**, *4*,

349.

[73] Y. Forterre, J. M. Skotheim, J. Dumais, L. Mahadevan, *Nature* **2005**, *433*, 421.

[74] E. Reyssat, L. Mahadevan, *J. R. Soc. Interface* **2009**, *6*, 951.

[75] S. Armon, E. Efrati, R. Kupferman, E. Sharon, *Science* **2011**, *333*, 1726.

[76] C. Somerville, S. Bauer, G. Brininstool, M. Facette, T. Hamann, J. Milne, E. Osborne, A. Paredez, S. Persson, T. Raab, S. Vorwerk, H. Youngs, *Science* **2004**, *306*, 2206.

[77] L. I. U. Wang-yu, Z. Yong, *Adv. Nat. Sci.* **2010**, *3*, 82.

[78] W. Tian, Z. Yang, Q. Zhang, J. Wang, M. Li, Y. Ma, Q. Cong, *Appl. Bionics Biomech.* **2017**, *2017*, DOI 10.1155/2017/8504638.

[79] S. Madala, R. F. Boehm, *Renew. Sustain. Energy Rev.* **2017**, *71*, 309.

[80] A. Kasaeian, G. Nouri, P. Ranjbaran, D. Wen, *Energy Convers. Manag.* **2018**, *156*, 688.

[81] Q. Ge, A. H. Sakhaei, H. Lee, C. K. Dunn, N. X. Fang, M. L. Dunn, *Sci. Rep.* **2016**, *6*, 1.

[82] C. M. Yakacki, R. Shandas, C. Lanning, B. Rech, A. Eckstein, K. Gall, *Biomaterials* **2007**, *28*, 2255.

[83] V. Srivastava, S. A. Chester, L. Anand, *J. Mech. Phys. Solids* **2010**, *58*, 1100.

[84] N. R. Khatri, M. N. Islam, P. Cao, R. C. Advincula, W. Choi, Y. Jiang, *Addit. Manuf.* **2021**, *48*, 102419.

[85] H. Kim, F. Torres, D. Villagran, C. Stewart, Y. Lin, T. L. B. Tseng, *Macromol. Mater. Eng.* **2017**, *302*, 1.

[86] S. Bodkhe, P. S. M. Rajesh, F. P. Gosselin, D. Therriault, *ACS Appl. Energy Mater.* **2018**, *1*, 2474.

[87] C. Liu, N. Huang, F. Xu, J. Tong, Z. Chen, X. Gui, Y. Fu, C. Lao, **2018**, 1.

[88] X. Wei, Y. Liu, D. Zhao, S. S. Ge, *J. Eur. Ceram. Soc.* **2020**, *40*, 5423.

[89] Y. Li, Y. A. Samad, K. Liao, *J. Mater. Chem. A* **2015**, *3*, 2181.

[90] Z. C. Kennedy, J. F. Christ, K. A. Evans, B. W. Arey, L. E. Sweet, M. G. Warner, R. L. Erikson, C. A. Barrett, *Nanoscale* **2017**, *9*, 5458.

[91] Y. Zeng, L. Jiang, Y. Sun, Y. Yang, Y. Quan, S. Wei, *Micromachines* **2020**, *11*, 713.

[92] L. Xie, X. Huang, K. Yang, S. Li, P. Jiang, *J. Mater. Chem. A* **2014**, *2*, 5244.

[93] C. Wan, C. R. Bowen, *J. Mater. Chem. A* **2017**, *5*, 3091.

[94] C. C. Bowland, M. H. Malakooti, H. A. Sodano, *ACS Appl. Mater. Interfaces* **2017**, *9*, 4057.

[95] Z. Zhou, C. C. Bowland, M. H. Malakooti, H. Tang, H. A. Sodano, *Nanoscale* **2016**, *8*, 5098.

[96] H. Kim, B. R. Wilburn, E. Castro, C. A. Garcia Rosales, L. A. Chavez, T. L. B. Tseng, Y. Lin, *J. Compos. Mater.* **2019**, *53*, 1319.

[97] A. Salimi, A. A. Yousefi, *J. Polym. Sci. Part B Polym. Phys.* **2004**, *42*, 3487.

[98] D. M. Correia, C. Ribeiro, V. Sencadas, L. Vikingsson, M. Oliver Gasch, J. L. Gómez Ribelles, G. Botelho, S. Lanceros-Méndez, *Mater. Des.* **2016**, *92*, 674.

[99] J. S. Han, C. W. Gal, J. H. Kim, S. J. Park, *Ceram. Int.* **2016**, *42*, 9475.

[100] Z. Guo, E. Nilsson, M. Rigdahl, B. Hagström, *J. Appl. Polym. Sci.* **2013**, *130*, 2603.

[101] S. J. Kang, Y. J. Park, J. Sung, P. S. Jo, C. Park, K. J. Kim, B. O. Cho, *Appl. Phys. Lett.* **2008**, *92*, DOI 10.1063/1.2830701.

[102] J. C. C. Ferreira, T. S. Monteiro, A. C. Lopes, C. M. Costa, M. M. Silva, A. V. Machado, S. Lanceros-Mendez, *J. Non. Cryst. Solids* **2015**, *412*, 16.

[103] C. Seoul, Y. T. Kim, C. K. Baek, *J. Polym. Sci. Part B Polym. Phys.* **2003**, *41*, 1572.

[104] H. J. Lee, S. Zhang, Y. Bar-Cohen, S. Sherrit, *Sensors (Switzerland)* **2014**, *14*, 14526.

[105] D. Remiens, E. Cattan, C. Soyer, T. Haccart, *Mater. Sci. Semicond. Process.* **2002**, *5*, 123.

[106] H. Cui, R. Hensleigh, D. Yao, D. Maurya, P. Kumar, M. G. Kang, S. Priya, X. (Rayne) Zheng, *Nat. Mater.* **2019**, *18*, 234.

[107] M. Nadgorny, A. Ameli, *ACS Appl. Mater. Interfaces* **2018**, *10*, 17489.

[108] Z. Chen, X. Song, L. Lei, X. Chen, C. Fei, C. T. Chiu, X. Qian, T. Ma, Y. Yang, K. Shung, Y. Chen, Q. Zhou, *Nano Energy* **2016**, *27*, 78.

[109] Z. Chen, X. Qian, X. Song, Q. Jiang, R. Huang, Y. Yang, R. Li, K. Shung, Y. Chen, Q. Zhou, *Micromachines* **2019**, *10*, DOI 10.3390/mi10030170.

[110] B. Tiller, A. Reid, B. Zhu, J. Guerreiro, R. Domingo-Roca, J. Curt Jackson, J. F. C. Windmill, *Mater. Des.* **2019**, *165*, 107593.

[111] H. Kim, T. Fernando, M. Li, Y. Lin, T. L. B. Tseng, *J. Compos. Mater.* **2018**, *52*, 197.

[112] S. Tagliaferri, A. Panagiotopoulos, C. Mattevi, *Mater. Adv.* **2021**, *2*, 540.

[113] H. Kim, A. Renteria-Marquez, M. D. Islam, L. A. Chavez, C. A. Garcia Rosales, M. A. Ahsan, T. L. B. Tseng, N. D. Love, Y. Lin, *J. Am. Ceram. Soc.* **2019**, *102*, 3685.

[114] K. Kim, W. Zhu, X. Qu, C. Aaronson, W. R. McCall, S. Chen, D. J. Sirbuly, *ACS Nano* **2014**, *8*, 9799.

[115] C. Lee, J. A. Tarbutton, *Procedia Manuf.* **2015**, *1*, 320.

[116] C. Shuai, G. Liu, Y. Yang, F. Qi, S. Peng, W. Yang, C. He, G. Wang, G. Qian, *Nano Energy* **2020**, *74*, 104825.

[117] *Ceram. Int.* **2015**, *41*, 6610.

[118] W. S. Kang, J. H. Koh, *J. Eur. Ceram. Soc.* **2015**, *35*, 2057.

[119] J. Kim, J. H. Koh, *J. Eur. Ceram. Soc.* **2015**, *35*, 3819.

[120] W. Choi, K. Choi, G. Yang, J. C. Kim, C. Yu, *Polym. Test.* **2016**, *53*, 143.

[121] S. K. Karan, D. Mandal, B. B. Khatua, *Nanoscale* **2015**, *7*, 10655.

[122] W. S. Jung, Y. H. Do, M. G. Kang, C. Y. Kang, *Curr. Appl. Phys.* **2013**, *13*, S131.

[123] K. Il Park, M. Lee, Y. Liu, S. Moon, G. T. Hwang, G. Zhu, J. E. Kim, S. O. Kim, D. K. Kim, Z. L. Wang, K. J. Lee, *Adv. Mater.* **2012**, *24*, 2999.

[124] S. H. Shin, Y. H. Kim, M. H. Lee, J. Y. Jung, J. Nah, *ACS Nano* **2014**, *8*, 2766.

[125] D. Chen, T. Sharma, J. X. J. Zhang, *Sensors Actuators, A Phys.* **2014**, *216*, 196.

[126] Y. K. Fuh, P. C. Chen, Z. M. Huang, H. C. Ho, *Nano Energy* **2015**, *11*, 671.

[127] X. Guan, B. Xu, J. Gong, *Nano Energy* **2020**, *70*, DOI 10.1016/j.nanoen.2020.104516.

[128] H. B. Kang, C. S. Han, J. C. Pyun, W. H. Ryu, C. Y. Kang, Y. S. Cho, *Compos. Sci.*

Technol. **2015**, *111*, 1.

[129] K. Il Park, S. Xu, Y. Liu, G. T. Hwang, S. J. L. Kang, Z. L. Wang, K. J. Lee, *Nano Lett.* **2010**, *10*, 4939.

[130] M. Zhang, T. Gao, J. Wang, J. Liao, Y. Qiu, H. Xue, Z. Shi, Z. Xiong, L. Chen, *Nano Energy* **2015**, *11*, 510.

[131] K. D. D. Willis, E. Brockmeyer, S. E. Hudson, I. Poupyrev, *UIST'12 - Proc. 25th Annu. ACM Symp. User Interface Softw. Technol.* **2012**, 589.

[132] R. Dogra, S. Rani, B. Sharma, in (Eds.: G.S. Hura, A.K. Singh, L. Siong Hoe), Springer Singapore, Singapore, **2021**, pp. 1339–1350.

[133] A. Leal-Junior, A. Frizera-Neto, C. Marques, M. J. Pontes, *Sensors* **2018**, *18*, DOI 10.3390/s18030916.

[134] Y. Qian, Y. Zhao, Q. Wu, Y. Yang, *Sensors Actuators B Chem.* **2018**, *260*, 86.

[135] F. M. Padilla, M. Gallardo, M. T. Peña-Fleitas, R. De Souza, R. B. Thompson, *Sensors* **2018**, *18*, DOI 10.3390/s18072083.

[136] L. Alwis, T. Sun, K. T. V Grattan, *Opt. Laser Technol.* **2016**, *78*, 62.

[137] Q. Zhao, F. Tian, X. Yang, S. Li, J. Zhang, X. Zhu, J. Yang, Z. Liu, Y. Zhang, T. Yuan, L. Yuan, *Optik (Stuttg).* **2017**, *133*, 60.

[138] K. Cook, J. Canning, S. Leon-Saval, Z. Reid, M. A. Hossain, J.-E. Comatti, Y. Luo, G.-D. Peng, *Opt. Lett.* **2015**, *40*, 3966.

[139] Y. Luo, J. Canning, J. Zhang, G.-D. Peng, *Opt. Fiber Technol.* **2020**, *58*, 102299.

[140] A. Sultangazin, J. Kusmangaliyev, A. Aitkulov, D. Akilbekova, M. Olivero, D. Tosi, *IEEE Sens. J.* **2017**, *17*, 6935.

[141] A. Aitkulov, D. Tosi, *IEEE Sens. J.* **2019**, *19*, 3282.

[142] C. W. Wu, C. Y. Kuo, J. W. Lin, C. C. Chiang, *Opt. Quantum Electron.* **2017**, *49*, 1.

[143] H. N. Chan, Y. Shu, B. Xiong, Y. Chen, Y. Chen, Q. Tian, S. A. Michael, B. Shen, H. Wu, *ACS Sensors* **2016**, *1*, 227.

[144] H. H. Hwang, W. Zhu, G. Victorine, N. Lawrence, S. Chen, *Small Methods* **2018**, *2*, 1.

[145] C. Tzivelekis, P. Sgardelis, K. Waldron, R. Whalley, D. Huo, K. Dalgarno, *PLoS One* **2020**, *15*, 1.

[146] Z. Dong, H. Cui, H. Zhang, F. Wang, X. Zhan, F. Mayer, B. Nestler, M. Wegener, P. A. Levkin, *Nat. Commun.* **2021**, *12*, 1.

[147] M. R. Khosravani, T. Reinicke, *Sensors Actuators, A Phys.* **2020**, *305*, 111916.

[148] L. Cevenini, M. M. Calabretta, G. Tarantino, E. Michelini, A. Roda, *Sensors Actuators, B Chem.* **2016**, *225*, 249.

[149] H. Ragones, D. Schreiber, A. Inberg, O. Berkh, G. Kósa, A. Freeman, Y. Shacham-Diamand, *Sensors Actuators B Chem.* **2015**, *216*, 434.

[150] A. H. Loo, C. K. Chua, M. Pumera, *Analyst* **2017**, *142*, 279.

[151] A. Roda, M. Guardigli, D. Calabria, M. Maddalena Calabretta, L. Cevenini, E. Michelini, *Analyst* **2014**, *139*, 6494.

[152] Z. Heger, J. Zitka, L. Nejdl, A. Moulick, V. Milosavljevic, P. Kopel, O. Zavodsky, J. Kapus, L. Lenza, M. Rezka, V. Adam, R. Kizek, *Monatshefte für Chemie - Chem. Mon.* **2016**, *147*, 873.

[153] T. Xiao, C. Qian, R. Yin, K. Wang, Y. Gao, F. Xuan, *Adv. Mater. Technol.* **2021**, *6*, 1.

[154] L. Zhang, G. Yang, B. N. Johnson, X. Jia, *Acta Biomater.* **2019**, *84*, 16.